Clim. Past, 14, 1361–1375, 2018
https://doi.org/10.5194/cp-14-1361-2018

Climate of the Past
Open Access
EGU

Last interglacial ocean changes in the Bahamas: climate teleconnections between low and high latitudes

Anastasia Zhuravleva[1] **and Henning A. Bauch**[2]

[1]Academy of Sciences, Humanities and Literature, Mainz c/o GEOMAR Helmholtz Centre for Ocean Research, Wischhofstrasse 1–3, Kiel, 24148, Germany
[2]Alfred Wegener Institute, Helmholtz Centre for Polar and Marine Research c/o GEOMAR Helmholtz Centre for Ocean Research, Wischhofstrasse 1–3, Kiel, 24148, Germany

Correspondence: Anastasia Zhuravleva (azhuravleva@geomar.de)

Received: 26 March 2018 – Discussion started: 11 April 2018
Revised: 29 August 2018 – Accepted: 10 September 2018 – Published: 1 October 2018

Abstract. Paleorecords and modeling studies suggest that instabilities in the Atlantic Meridional Overturning Circulation (AMOC) strongly affect the low-latitude climate, namely via feedbacks on the Atlantic Intertropical Convergence Zone (ITCZ). Despite the pronounced millennial-scale overturning and climatic variability documented in the subpolar North Atlantic during the last interglacial period (MIS 5e), studies on cross-latitudinal teleconnections remain very limited. This precludes a full understanding of the mechanisms controlling subtropical climate evolution across the last warm cycle. Here, we present new planktic foraminiferal assemblage data combined with δ^{18}O values in surface and thermocline-dwelling foraminifera from the Bahamas, a region ideally suited to studying past changes in the subtropical ocean and atmosphere. Our data reveal that the peak sea surface warmth during early MIS 5e was intersected by an abrupt millennial-scale cooling/salinification event, which was possibly associated with a sudden southward displacement of the mean annual ITCZ position. This atmospheric shift is, in turn, ascribed to the transitional climatic regime of early MIS 5e, which was characterized by persistent ocean freshening in the high latitudes and an unstable AMOC mode.

1 Introduction

In the low-latitude North Atlantic, wind patterns, the precipitation–evaporation balance, sea surface temperatures (SSTs) and sea surface salinities (SSSs) are strongly dependent on the position of the Atlantic Intertropical Convergence Zone (ITCZ) and its associated rainfall (Peterson and Haug, 2006). Based on paleorecords and modeling studies, past positions of the ITCZ are thought to be related to the interhemispheric thermal contrast (Schneider et al., 2014). In turn, changes in the thermal contrast could be principally driven by two mechanisms: (1) the precessional cycle and the associated cross-latitudinal distribution of solar insolation, or (2) the millennial-scale climatic variability brought about by Atlantic Meridional Overturning Circulation (AMOC) instabilities (Wang et al., 2004; Broccoli et al., 2006; Arbuszewski et al., 2013; Schneider et al., 2014). Specifically, millennial-scale cold events in the high northern latitudes were linked with reduced convection rates of the AMOC, accounting for both a decreased oceanic transport of tropical heat towards the north and a southward shift of the mean annual position of the ITCZ (Vellinga and Wood, 2002; Chiang et al., 2003; Broccoli et al., 2006). Reconstructions from the low-latitude North Atlantic confirm southward displacements of the ITCZ coeval with AMOC reductions and reveal a complex hydrographic response within the upper water column, generally suggesting an accumulation of heat and salt in the (sub)tropics (Schmidt et al., 2006a; Carlson et al., 2008; Bahr et al., 2011, 2013). However, there are opposing views on the subtropical sea surface development at times of high-latitude cooling events. While some studies suggest stable or increasing SSTs (Schmidt et al., 2006a; Bahr et al., 2011, 2013), others imply an atmospheric-induced (evaporative) cooling (Chang et al., 2008; Chiang et al., 2008).

The last interglacial (MIS 5e), which lasted from about ∼ 130 to 115 thousand years before present (hereafter [ka]),

is often referred to as a "warmer than preindustrial" interval (Hoffman et al., 2017). This period was associated with significantly reduced ice sheets and a sea level rise up to 6–9 m above the present levels (Dutton et al., 2015). MIS 5e has also attracted a lot of attention as a possible analog for future climatic development as well as a critical target for validation of climatic models (Masson-Delmotte et al., 2013). Proxy data from the North Atlantic demonstrate that the climate of the last interglacial was relatively unstable, involving one or several cooling events (Maslin et al., 1998; Fronval and Jansen, 1997; Bauch et al., 2012; Irvalı et al., 2012, 2016; Zhuravleva et al., 2017a, b). This climatic variability is thought to be strongly related to changes in the AMOC strength (Adkins et al., 1997). Thus, recent studies reveal that the AMOC abruptly recovered after MIS 6 deglaciation (Termination 2 or T2), i.e., at the onset of MIS 5e, at $\sim$ 129 ka, but it was interrupted around 127–126 ka (Galaasen et al., 2014; Deaney et al., 2017). Despite the pronounced millennial-scale climatic variability documented in the high northern latitudes, studies on the cross-latitudinal links are very limited (see e.g., Cortijo et al., 1999; Schwab et al., 2013; Kandiano et al., 2014; Govin et al., 2015; Jiménez-Amat and Zahn, 2015). This precludes a full understanding of the mechanisms (e.g., insolation, oceanic and/or atmospheric forcing versus high-to-low-latitude climate feedbacks) regulating subtropical climate across the last interglacial.

Given its critical location near the origin of the Gulf Stream, sediments from the slopes of the shallow-water carbonate platforms of the Bahamian archipelago (Fig. 1) have been previously investigated in terms of oceanic and atmospheric variability (Slowey and Curry, 1995; Roth and Reijmer, 2004, 2005; Chabaud et al., 2016). However, a thorough study of the last interglacial climatic evolution underpinned by a critical stratigraphical insight is lacking to date. Here, a sediment record from the Little Bahama Bank (LBB) region is investigated for possible links between the AMOC variability and the ITCZ during the last interglacial cycle. Today the LBB region lies at the northern edge of the influence of the Atlantic Warm Pool, which has expansion that is strongly related to the ITCZ movements (Wang and Lee, 2007; Levitus et al., 2013), making our site particularly sensitive regarding monitoring past shifts of the ITCZ. Given that geochemical properties of marine sediments around carbonate platforms vary in response to sea level fluctuations (e.g., Lantzsch et al., 2007), X-ray fluorescence (XRF) data are being used in combination with stable isotope and faunal records to strengthen the temporal framework. Planktic foraminiferal assemblage data complemented by δ^{18}O values, measured on surface- and thermocline-dwelling foraminifera, are employed to reconstruct the upper ocean properties (stratification, trends in temperature and salinity), specifically looking at mechanisms controlling the foraminiferal assemblages. Assuming a coupling between foraminiferal assemblage data and past mean annual positions of the ITCZ (Poore et al., 2003; Vautravers et al., 2007), our faunal records are then viewed in terms of potential geographical shifts of the ITCZ. Finally, we compare our new proxy records with published evidence from the regions of deep water formation to draw further conclusions on the subpolar forcing on the low-latitude climate during MIS 5e.

2 Regional setting

2.1 Hydrographic context

Core MD99-2202 (27°34.5′ N, 78°57.9′ W, 460 m water depth) was taken from the upper northern slope of the LBB, which is the northernmost shallow-water carbonate platform of the Bahamian archipelago. The study area is at the western boundary of the wind-driven subtropical gyre (STG), in the vicinity of the Gulf Stream (Fig. 1a), which supplies both heat and salt to the high northern latitudes and constitutes the upper cell of the AMOC.

In the western subtropical North Atlantic two distinctly different layers can be distinguished within the upper 500 m of the water column (Fig. 1c). The uppermost mixed layer (upper 50–100 m) is occupied by warm and comparatively fresh waters ($T > 24$ °C, $S < 36.4$ psu), which predominantly come from the equatorial Atlantic (Schmitz and McCartney, 1993; Johns et al., 2002). Properties of this water mass vary significantly on seasonal timescales and are closely related to the latitudinal migration of the ICTZ (Fig. 1b). During boreal winter (December–April), when the ITCZ is in its southernmost position, the Bahama region is dominated by relatively cool, stormy weather with prevailing northern and northeastern trade winds and is affected by cold western fronts, which increase evaporation and vertical convective mixing (e.g., Wilson and Roberts, 1995). During the May to November period, as the ITCZ moves northward, the LBB region is influenced by relatively weakened trade winds from the east and southeast, increased precipitation and the very warm waters of the Atlantic Warm Pool ($T > 28.5$ °C), which expand into the Bahama region from the Caribbean Sea and the equatorial Atlantic (Stramma and Schott, 1999; Wang and Lee, 2007; Levitus et al., 2013).

The mixed layer is underlain by the permanent thermocline, which is comprised of a homogeneous pool of comparatively cool and salty ($T < 24$ °C, $S > 36.4$ psu) water (Schmitz and Richardson, 1991). These "mode" waters are formed in the North Atlantic STG through wintertime subduction of surface waters generated by wind-driven Ekman downwelling and buoyancy flux (Slowey and Curry, 1995).

2.2 Sedimentological context

Along the slopes of the LBB, sediments are composed of varying amounts of sedimentary input from the top of the platform and from the open ocean, depending on the global sea level state (Droxler and Schlager, 1985; Schlager et al., 1994). During interglacial highstands, when the platform is

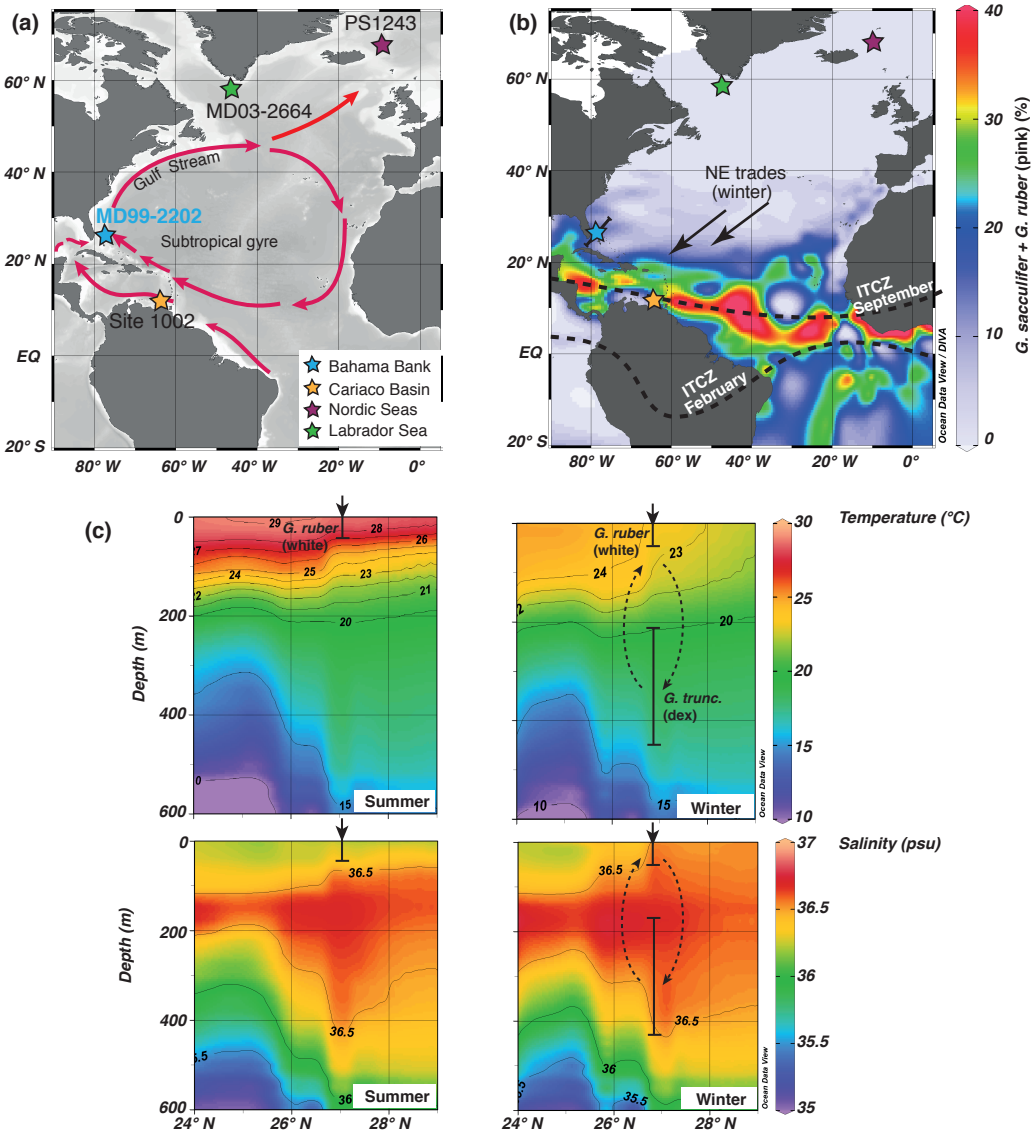

Figure 1. Maps showing the positions of investigated sediment records and oceanic/atmospheric circulation. **(a)** Simplified surface water circulation in the (sub)tropical North Atlantic and the positions of the core records investigated: MD99-2202 (27°34.5′ N, 78°57.9′ W, 460 m water depth; this study), Ocean Drilling Program (ODP) Site 1002 (10°42.7′ N, 65°10.2′ W, 893 m water depth; Gibson and Peterson, 2014), MD03-2664 (57°26.3′ N, 48°36.4′ W, 3442 m water depth, Galaasen et al., 2014) and PS1243 (69°22.3′ N, 06°33.2′ W, 2710 m water depth, Bauch et al., 2012). **(b)** Relative abundances of the tropical foraminifera *G. sacculifer* and *G. ruber* (pink) (Siccha and Kučera, 2017) and positions of the Intertropical Convergence Zone (ITCZ) during boreal winter and summer. **(c)** Summer and winter hydrographic sections (as defined by the black line in **b**), showing temperature and salinity obtained from the World Ocean Atlas (Levitus et al., 2013). Vertical bars denote the calcification depths of *G. ruber* (white) and *G. truncatulinoides* (dex). Note that *G. truncatulinoides* (dex) reproduces in wintertime and due to its life cycle with changing habitats (as shown with arrows) it accumulates signals from different water depths. Maps were created using Ocean Data View (Schlitzer, 2017).

submerged, the major source of sediment input is the downslope transport of fine-grained aragonite needles, precipitated on the top of the platform. This material incorporates significantly higher abundances of strontium (Sr), than found in pelagic-derived aragonite (e.g., pteropods) and calcite material from planktic foraminifera and coccoliths (Morse and MacKenzie, 1990). Given that in the periplatform interglacial environment modifications of the aragonite content due to sea floor dissolution and/or winnowing of fine-grained material are minimal (Droxler and Schlager, 1985; Schlager et al., 1994; Slowey et al., 2002), thicker sediment packages accumulate on the slopes of the platform, yielding interglacial

climate records of high resolution (Roth and Reijmer, 2004, 2005). During glacial lowstands, on the contrary, as the platform is exposed, aragonite production is limited, sedimentation rates are strongly reduced and coarser-grained consolidated sediments are formed from the pelagic organisms (Droxler and Schlager, 1985; Slowey et al., 2002; Lantzsch et al., 2007).

3 Methods

3.1 Foraminiferal counts and stable isotope analyses

Planktic foraminiferal assemblages were counted on representative splits of the 150–250 µm fraction containing at least 300 individual specimens. Counts were also performed in the >250 µm fraction. The census data from the two size fractions were summed and recalculated into the relative abundance of planktic foraminifera in the >150 µm fraction. Faunal data were obtained at each 2 cm interval for the core section between 508.5 and 244.5 cm and at each 10 cm interval between 240.5 and 150.5 cm. According to a standard practice, *Globorotalia menardii* and *Globorotalia tumida* as well as *Globigerinoides sacculifer* and *Globigerinoides trilobus* were grouped together; these groups were referred to as *G. menardii* and *G. sacculifer*, respectively (Poore et al., 2003; Kandiano et al., 2012; Jentzen et al., 2018).

New oxygen isotope data were produced at 2 cm steps using ∼ 10–30 tests of *Globorotalia truncatulinoides* (dex) and ∼ 5-20 tests of *Globorotalia inflata* for depth intervals of 508.5–244.5 and 508.5–420.5 cm, respectively. Analyses were performed using a Finnigan MAT 253 mass spectrometer at the GEOMAR Stable Isotope Laboratory. Calibration to the Vienna Pee Dee Belemnite (VPDB) isotope scale was made via the NBS-19 and an internal laboratory standard. The analytical precision of the in-house standard was better than 0.07 ‰ (1σ) for δ^{18}O.

Isotopic data derived from the deep-dwelling foraminifera *G. truncatulinoides* (dex) and *G. inflata* could be largely associated with the permanent thermocline and linked to winter conditions (Groeneveld and Chiessi, 2011; Jonkers and Kučera, 2015; Jentzen et al., 2018). However, as calcification of their tests is already apparent in the mixed layer and continues in the main thermocline (Fig. 1c), the abovementioned species are thought to accumulate hydrographic signals from different water depths in their tests (Groeneveld and Chiessi, 2011; Mulitza et al., 1997).

3.2 XRF scanning

XRF analysis was performed in two different runs using the Aavatech XRF Core Scanner at Christian-Albrecht University of Kiel (for technical details see Richter et al., 2006). To obtain the intensities of elements with lower atomic weight (e.g., calcium (Ca) and chlorine (Cl)), XRF scanning measurements were carried out with an X-ray tube voltage of 10 kv, a tube current of 750 µA and a counting time of 10 s. To analyze heavy elements (e.g., iron (Fe) and Sr), an X-ray generator setting of 30 kv and 2000 µA and a counting time of 20 s were used; a thick palladium filter was placed in the X-ray tube to reduce the high background radiation generated by the higher source energies. XRF Core Scanner data were collected directly from the split core sediment surface, which had been flattened and covered with a 4 µm-thick ULTRALENE SPEXCerti Prep film to prevent the contamination of the measurement unit and desiccation of the sediment (Richter et al., 2006; Tjallingii et al., 2007). The core section between 150 and 465 cm was scanned at a step size of 3 mm, whereas the coarser-grained interval between 465 and 600 cm was analyzed at a 10 mm resolution.

To account for potential biases related to the physical properties of the sediment core (see e.g., Chabaud, 2016), XRF intensities of Sr were normalized to Ca, the raw total counts of Fe and Sr were normalized to the total counts of the 30 kv run; counts of Ca and Cl were normalized to the total counts of the 10 kv run, excluding rhodium intensity, as the intensities of these elements are biased by the signal generation (Bahr et al., 2014).

4 Age model

By using our foraminiferal assemblage data, we were able to refine the previously published age model of core MD99-2202 (Lantzsch et al., 2007). To correctly frame MIS 5e, stratigraphic subdivision of the unconsolidated aragonite (Sr)-rich sediment package between 190 and 464 cm is essential (Fig. 2). In agreement with Lantzsch et al. (2007), we interpret this core section as comprising MIS 5, which is supported by key biostratigraphic markers used to identify the well-established faunal zones of the late Quaternary (Ericson and Wollin, 1968). Thus, the last occurrence of *G. menardii* at the end of the aragonite-rich sediment package is in agreement with the estimated late MIS 5 age (ca. 80–90 ka; Boli and Saunders, 1985; Slowey et al., 2002; Bahr et al., 2011; Chabaud, 2016). The coherent variability in the ∼ 200–300 cm core interval, observed between the aragonite content and the relative abundances of warm surface-dwelling foraminifera of the *Globigerinoides* genus (*G. ruber*, white and pink varieties, *G. conglobatus* and *G. sacculifer*), points to simultaneous climate and sea level related changes and likely reflects the warm/cold substages of MIS 5. The identified substages were then correlated with the global isotope benthic stack LS16 (Lisiecki and Stern, 2016) using AnalySeries 2.0.8 (Paillard et al., 1996). Further, boundaries between MIS 6/5e and 5e/5d as well as the penultimate glaciation (MIS 6) peak, defined from the δ^{18}O record of *G. ruber* (white), were aligned to the global benthic stack (Lisiecki and Stern, 2016).

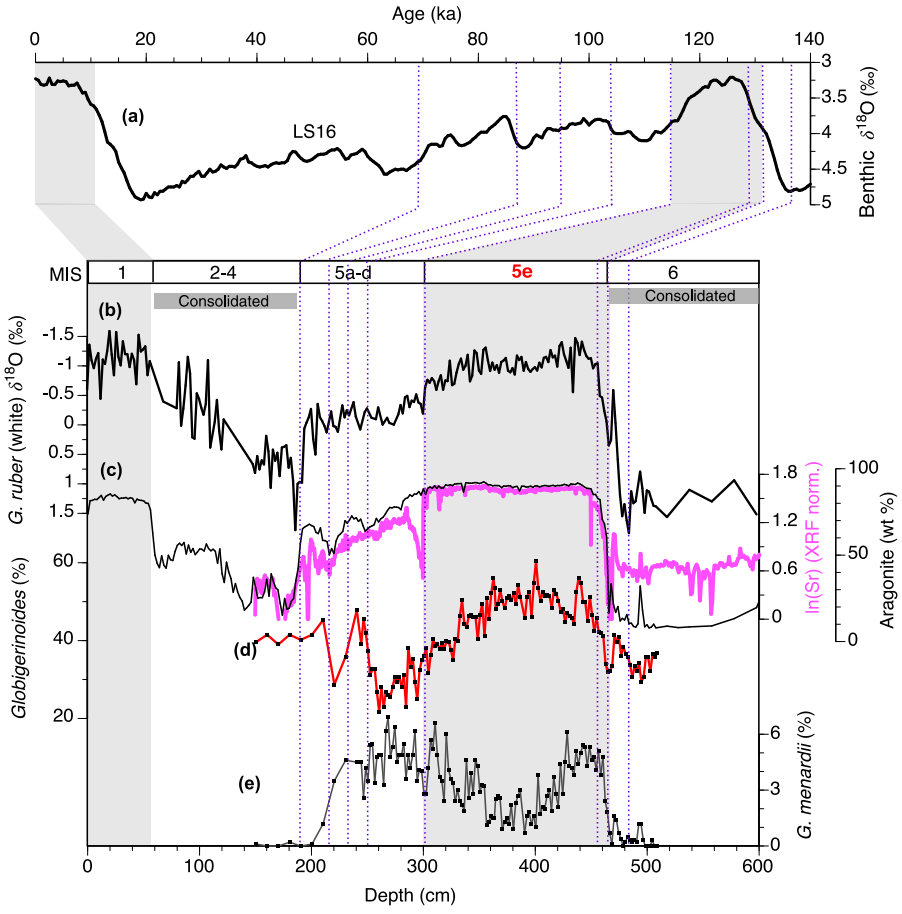

Figure 2. The age model for MIS 5 in core MD99-2202. The temporal framework is based on the alignment of **(b)** planktic δ^{18}O values (Lantzsch et al., 2007) and **(d)** the relative abundance record of *Globigerinoides* species with **(a)** global benthic isotope stack LS16 (Lisiecki and Stern, 2016). **(c)** Aragonite content (in black; Lantzsch et al., 2007) and normalized elemental intensities of Sr (in magenta) as well as **(e)** relative abundances of *G. menardii* are shown to support the stratigraphic subdivision of MIS 5.

Given that sedimentation rates at the glacial/interglacial transition could have changed drastically due to the increased production of Sr-rich aragonite material above the initially flooded carbonate platform top (Roth and Reijmer, 2004), we applied an additional age marker to better frame the onset of the MIS 5e "plateau" (Masson-Delmotte et al., 2013) and to allow for a better core-to-core comparison. Thus, we tied the increased relative abundances of warm surface-dwelling foraminifera of the *Globigerinoides* genus, which coincides with the rapid decrease in the foraminiferal δ^{18}O record at 456 cm, with the onset of the MIS 5e "plateau" at $\sim$ 129 ka (Masson-Delmotte et al., 2013). This age is in good agreement with many marine and speleothem records, dating a rapid post-stadial warming and monsoon intensification to 129–128.7 ka (Govin et al., 2015; Jiménez-Amat and Zahn, 2015; Deaney et al., 2017), which is coincident with the sharp methane increase in the EPICA Dome C ice core (Loulergue et al., 2008; Govin et al., 2012). Although we do not apply a specific age marker to frame the decline of the MIS 5e "plateau", the resulting decrease in the percentage of warm surface-dwelling foraminifera of the *Globigerinoides* genus as well as the initial increase in the planktic δ^{18}O values dates back to $\sim$ 117 ka (Figs. 3–5), which broadly coincides with the cooling onset over Greenland (NGRIP community members, 2004). A similar subtropical–polar climatic coupling was proposed in earlier studies from the western North Atlantic STG (e.g., Vautravers et al., 2004; Schmidt et al., 2006a; Bahr et al., 2013; Deaney et al., 2017).

5 Results

5.1 XRF data in the lithological context

In Fig. 3, XRF-derived elemental data are plotted against lithological and sedimentological records. Beyond the intervals with low Ca counts and correspondingly high Cl intensities (at 300–325 and 395–440 cm), Ca intensities do not vary significantly, which is in line with a stable carbonate content of about 94 % wt, revealed by Lantzsch et al. (2007). Our

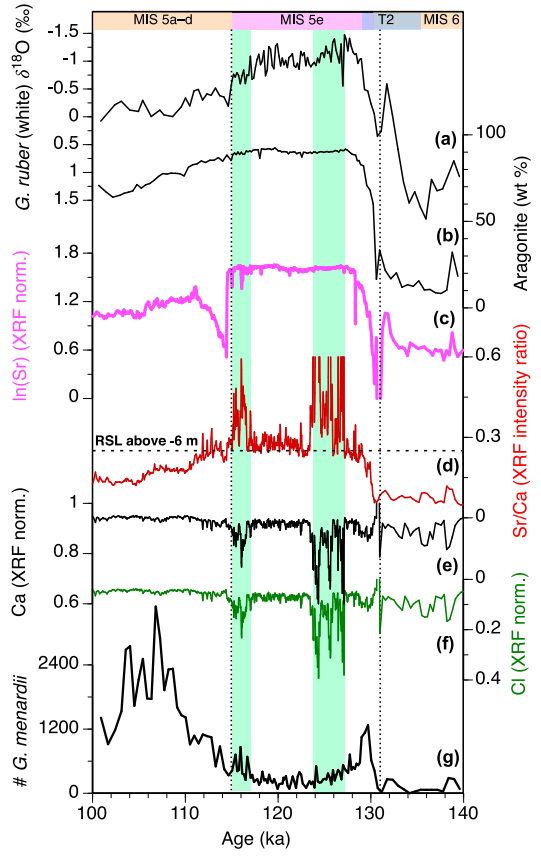

Figure 3. XRF-scan results, sedimentological and foraminiferal data from core MD99-2202 for the 140–100 ka period. **(a)** δ^{18}O values in *G. ruber* (white) and **(b)** aragonite content; **(a–b)** is from Lantzsch et al. (2007). Normalized elemental intensities of **(c)** Sr, **(e)** Ca and **(f)** Cl, **(d)** Sr/Ca intensity ratio (truncated at 0.6) and **(g)** absolute abundances of *G. menardii* per sample. Green bars denote core intervals with biased elemental intensities due to high seawater content. The inferred platform flooding interval (see text) is consistent with the enhanced production of Sr-rich aragonite needles and a RSL above −6 m **(d)**. T2 refers to the position of the penultimate deglaciation (Termination 2). Dashed vertical lines frame MIS 5e.

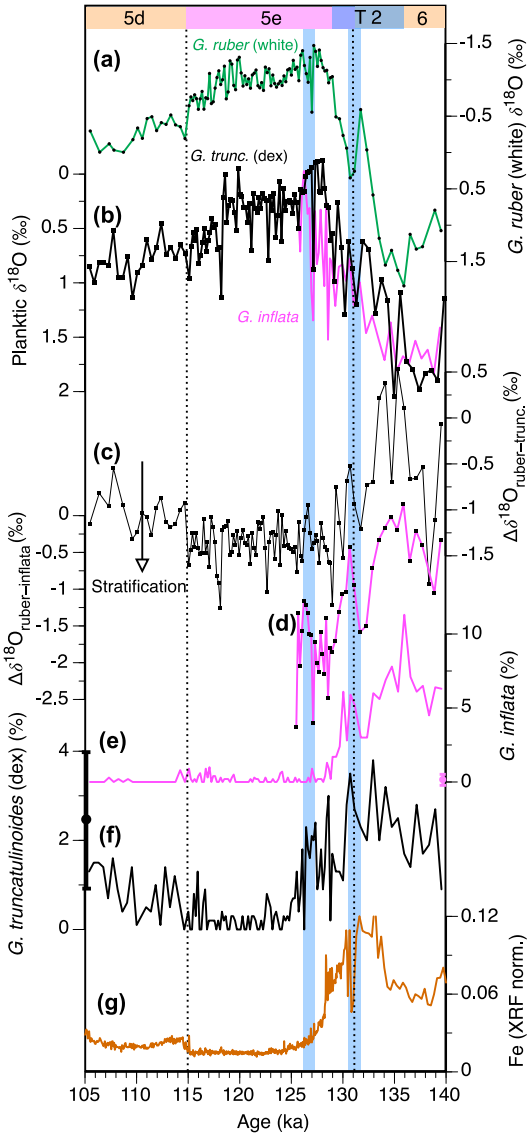

Figure 4. Proxy records from core MD99-2202 over the last interglacial cycle. **(a)** δ^{18}O values in *G. ruber* (white) (Lantzsch et al., 2007); **(b)** δ^{18}O values in *G. truncatulinoides* (dex) (in black) and *G. inflata* (in magenta); **(c–d)** isotopic gradients between δ^{18}O values in *G. ruber* (white) and *G. truncatulinoides* (dex) and *G. ruber* (white) and *G. inflata*, respectively; **(e–f)** relative abundances of *G. inflata* and *G. truncatulinoides* (dex), respectively; and **(g)** normalized Fe intensities. Also shown in **(e)** and **(f)** are the modern relative foraminiferal abundances (average value $\pm 1\sigma$) around Bahama Bank, computed using the seven nearest samples from the Siccha and Kučera (2017) database. Vertical blue bars represent periods of decreased water column stratification, discussed in the text. Dashed vertical lines frame MIS 5e. T2 represents Termination 2.

Sr record closely follows the aragonite curve, demonstrating that the interglacial mineralogy is dominated by aragonite. Beyond the intervals containing reduced Ca intensities, a good coherence between Sr/Ca and aragonite content is observed. The rapid increase in Sr/Ca and aragonite is found at the end of the penultimate deglaciation (T2), coeval with the elevated absolute abundances of *G. menardii* per sample (Fig. 3). The gradual step-like Sr/Ca and aragonite decrease characterizes both the glacial inception and the later MIS 5 phase. Intensities of Fe abruptly decrease at the beginning of the last interglacial, but gradually increase during the glacial inception (Fig. 4). Note that between ∼ 112 and 114.5 ka, the actual XRF measurements were affected by a low sediment level in the core tube.

5.2 Climate-related proxies

To calculate δ^{18}O gradients across the upper water column, we also used the published δ^{18}O data by Lantzsch et

al. (2007), which were measured on the surface-dwelling foraminifera *G. ruber* (white). These isotopic data can be generally associated with mean annual conditions (Tedesco et al., 2007); however, during colder time intervals the productivity peak of *G. ruber* (white) could shift towards warmer months, leading to an underestimation of the actual environmental change (Schmidt et al., 2006a, b; Jonkers and Kučera, 2015). During the penultimate glacial maximum (MIS 6), δ^{18}O gradients between *G. ruber* (white) and *G. truncatulinoides* (dex) and *G. inflata* are very low (Fig. 4), which is succeeded by a gradually increasing difference across T2, ∼ 135–129 ka. Changes in the isotopic gradient between surface- and thermocline-dwelling foraminifera closely follow variations in the relative abundances of *G. truncatulinoides* (dex) and *G. inflata* (Fig. 4). Across MIS 5e species of *Globigerinoides* genus dominate the total assemblage; however, significant changes in the proportions of three main *Globigerinoides* species are observed (Fig. 5): *G. sacculifer* and *G. ruber* (pink) essentially dominate the assemblage during early MIS 5e (129–124 ka), whereas *G. ruber* (white) proportions are at their maximum during late MIS 5e (124–117 ka). At around 127 ka, all δ^{18}O records abruptly increase in combination with the reappearance of *G. inflata* (Fig. 4) and a decrease in the relative abundance of *G. ruber* (pink) and *G. sacculifer* (Fig. 5). After 120 ka, δ^{18}O values in *G. ruber* (white) and *G. truncatulinoides* (dex) become variable (Fig. 4). That instability coincides with an abrupt drop in *G. sacculifer* relative abundances (Fig. 5).

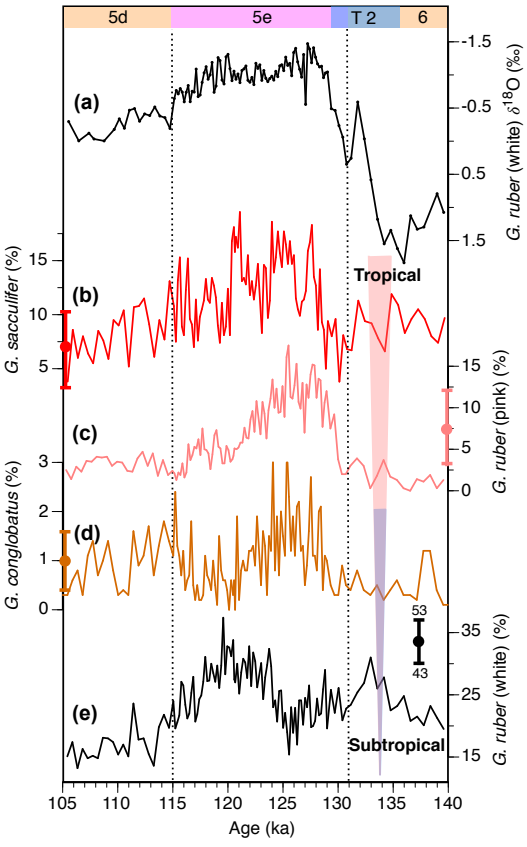

Figure 5. Relative abundances of the main *Globigerinoides* species in core MD99-2202 over the last interglacial cycle. **(a)** δ^{18}O values in *G. ruber* (white) (Lantzsch et al., 2007), relative abundances of **(b)** *G. sacculifer*, **(c)** *G. ruber* (pink), **(d)** *G. conglobatus* and **(e)** *G. ruber* (white). Also shown in **(b–e)** are the modern relative foraminiferal abundances (average value $\pm 1\sigma$) around Bahama Bank, computed using the seven nearest samples from the Siccha and Kučera (2017) database. Dashed vertical lines frame MIS 5e. T2 represents Termination 2.

6 Discussion

6.1 Platform sedimentology and relative sea level change

The modern LBB lagoon is shallow with an average water depth of between 6 and 10 m (Williams, 1985). Despite some possible isostatic subsidence of 1–2 m per hundred thousand years (Carew and Mylroie, 1995), the LBB region is generally regarded as tectonically stable (Hearty and Neumann, 2001). Considering this, a relative sea level (RSL) rise above −6 m of its present position is required to completely flood the top of the platform and allow for a drastic increase in platform-derived (Sr-rich aragonite) sediment particles (Neumann and Land, 1975; Droxler and Schlager, 1985; Schlager et al., 1994; Carew and Mylroie, 1997). As such, the LBB flooding periods exceeding −6 m RSL can be defined from downcore variations in Sr/Ca intensity ratio (Chabaud et al., 2016).

While our Sr record likely represents a non-affected signal because of good coherence with the aragonite record, some of the Ca intensity values are reduced due to increased seawater content, as evidenced by simultaneously measured elevated Cl intensities (Fig. 3). Because enhanced seawater content in the sediment appears to reduce only Ca intensities, which leaves elements of higher atomic order (e.g., Fe and Sr) less affected (Tjallingii et al., 2007; Hennekam and de Lange, 2012), the normalization of Sr counts to Ca results in very high Sr/Ca intensity ratios across the Cl-rich intervals. Regardless of these problematic intervals described above, the XRF-derived Sr/Ca values agree well with the measured aragonite values; therefore, it seems permissible to interpret these values in terms of RSL variability. Here, it should be noted that, although the Bahama region is located quite far from the former Laurentide Ice Sheet, there still could have been some influence from glacio-isostatic adjustments, which would have caused our RSL signals to deviate from the global sea level during MIS 5e (Stirling et al., 1998).

Around 129 ka, Sr/Ca rapidly increased, indicating the onset of the LBB flooding interval with the inferred RSL above −6 m (Fig. 3). The absolute abundance of *G. menardii* per sample supports the inferred onset of the flooding interval, as

amounts of planktic foraminifera in the sample can be used to assess the relative accumulation of platform-derived versus pelagic sediment particles (Slowey et al., 2002). Thus, after *G. menardii* repopulated the (sub)tropical waters at the end of the penultimate glaciation (Bahr et al., 2011; Chabaud, 2016), its increased absolute abundances are found around Bahamas between ∼ 130 and 129 ka. This feature could be attributed to the reduced input of fine-grained aragonite during the periods when the platform was partly flooded. Consequently, as the top of the platform became completely submerged, established aragonite shedding gained over pelagic input, thereby reducing the number of *G. menardii* per given sample. Our proxy records further suggest that the aragonite production on top of the platform was abundant until late MIS 5e (unequivocally delimited by foraminiferal δ^{18}O and faunal data). The drop in RSL below −6 m that only occurred during the terminal phase of MIS 5e (∼ 117–115 ka on our timescale) is corroborated by a coincident changeover in the aragonite content and an increase in the absolute abundance of *G. menardii*. This further supports the hypothesis that aragonite shedding was suppressed at that time, causing a relative enrichment in foraminiferal abundances.

6.2 Deglacial changes in the vertical water mass structure

Elevated proportions of thermocline-dwelling foraminifera *G. inflata* and *G. truncatulinoides* (dex) are found off the LBB during late MIS 6 and T2 (Fig. 4). To define mechanisms controlling the faunal assemblage, we look at δ^{18}O values in those foraminiferal species which document hydrographic changes across the upper water column, i.e., spanning from the uppermost mixed layer down to the permanent thermocline. The strongly reduced δ^{18}O gradients between surface-dwelling species *G. ruber* (white) and two thermocline-dwelling foraminifera *G. truncatulinoides* (dex) and *G. inflata* during T2 and particularly during late MIS 6 could be interpreted in terms of decreased water column stratification, a condition which is favored by thermocline-dwelling foraminifera (e.g., Mulitza et al., 1997). Specifically, for *G. truncatulinoides* (dex) this hypothesis is supported by its increased abundance within the regions characterized by deep winter vertical mixing (Siccha and Kučera, 2017). Such environmental preference may be explained by species ontogeny, given that *G. truncatulinoides* (dex) requires reduced upper water column stratification to be able to complete its reproduction cycle with habitats ranging from ca. 400 to 600 m to near-surface depths; however, in well-stratified waters reproduction of *G. truncatulinoides* (dex) would be inhibited by a strong thermocline (Lohmann and Schweizer, 1990; Hilbrecht, 1996; Mulitza et al., 1997; Schmuker and Schiebel, 2000).

To explain the inferred reduced upper water mass stratification during late MIS 6 and T2, sea surface cooling/salinification and/or subsurface warming could be invoked (e.g., Zhang, 2007; Chiang et al., 2008). While Mg/Ca-based temperature estimations during late MIS 6 so far reveal cold subsurface conditions for the subtropical western North Atlantic (Bahr et al., 2011, 2013), it should be noted that species-specific signals (i.e., δ^{18}O values, Mg/Ca-ratios) could be complicated due to the adaptation strategies of foraminifera, such as seasonal shifts in the peak foraminiferal tests flux and/or habitat changes (Schmidt et al., 2006a, b; Cléroux et al., 2007; Bahr et al., 2013; Jonkers and Kučera, 2015). However, further insights into the past fluctuations in seawater temperature and salinity could be provided from the conspicuous millennial-scale oscillation found at 131 ka (Fig. 4) and associated with a shift towards lower surface–thermocline isotopic gradients (i.e., reduced stratification). When compared to the abrupt increase in *G. ruber* (white) δ^{18}O values at 131 ka, which indicates sea surface cooling or salinification, the isotopic response in thermocline-dwelling species remains rather muted. The latter could either be explained by foraminiferal adaptation strategies, stable subsurface conditions and/or the incorporation of opposing signals during foraminiferal ontogenetic cycle that would mitigate the actual environmental change. Regardless of the exact mechanism, there is a good coherence between δ^{18}O values in *G. ruber* (white) and relative abundances of *G. inflata* and *G. truncatulinoides* (dex), suggesting a possible link between thermocline species abundance and conditions occurring nearer to the sea surface (Mulitza et al., 1997; Jonkers and Kučera, 2017). Specifically, steadily increasing upper water column stratification across the glacial–interglacial transition could have suppressed the reproduction of *G. truncatulinoides* (dex) and *G. inflata*, while the short-term stratification reduction at 131 ka may have promoted favorable conditions for the thermocline-dwelling species through sea surface cooling and/or salinification.

However, it should be noted that stratification is not the sole mechanism explaining the variability in the thermocline-associated assemblage. Thus, while relative abundances of *G. inflata* become strongly reduced at the onset of MIS 5e, there is no such response in the *G. truncatulinoides* (dex) proportions (Fig. 4). Furthermore, *G. inflata* is generally regarded as a subpolar to transitional species, preferring little seasonal variations in salinity (Hilbrecht, 1996), whilst *G. truncatulinoides* (dex) has been shown to dwell in warmer temperatures (Siccha and Kučera, 2017) and also occurs in small amounts in the modern tropical Atlantic (Jentzen et al., 2018). However, an abrupt increase in the proportions of the latter species during the sea surface cooling/salinification event at ∼ 127 ka (discussed further below), coupled with reduced upper water column stratification, supports the underlying "sea surface" control on the general abundance of *G. truncatulinoides* (dex).

A southern position of the mean annual ITCZ during the penultimate (de)glaciation could be inferred based on previous studies (Yarincik et al., 2000; Wang et al., 2004; Schmidt

et al., 2006a; Carlson et al., 2008; Arbuszewski et al., 2013; Bahr et al., 2013). By analogy with the modern atmospheric forcing in the region, southern positioning of the ITCZ could have caused enhanced upper water column mixing and evaporative cooling through intensified trade winds (e.g., Wilson and Roberts, 1995). Acknowledging the fact that our study region lies too far north to be influenced by changes in the winter position of the ITCZ (Ziegler et al., 2008) – this would be of primary importance for winter–spring reproduction timing of *G. truncatulinoides* (dex) and *G. inflata* as is currently the case (Jonkers and Kučera, 2015) – we suggest that a southern location of the mean annual position of the ITCZ during the penultimate (de)glaciation could have facilitated favorable conditions for the latter species through generally strong sea surface cooling/salinification in the subtropical North Atlantic.

Previous studies have attributed the increased Fe content in the Bahamas sediments to enhanced trade wind strength, given that siliciclastic inputs by processes other than wind transport are very limited (Roth and Reijmer, 2004). Accordingly, elevated XRF-derived Fe counts in our record during T2 (Fig. 4) may support the intensification of the trade winds and possibly increased transport of Saharan dust at times of enhanced aridity over northern Africa (Muhs et al., 2007; Helmke et al., 2008). However, we refrain from further interpretations of our XRF record due to a variety of additional effects that may have influenced our Fe-record (e.g., diagenesis, change in sources and/or properties of eolian inputs, and sensitivity of the study region to atmospheric shifts).

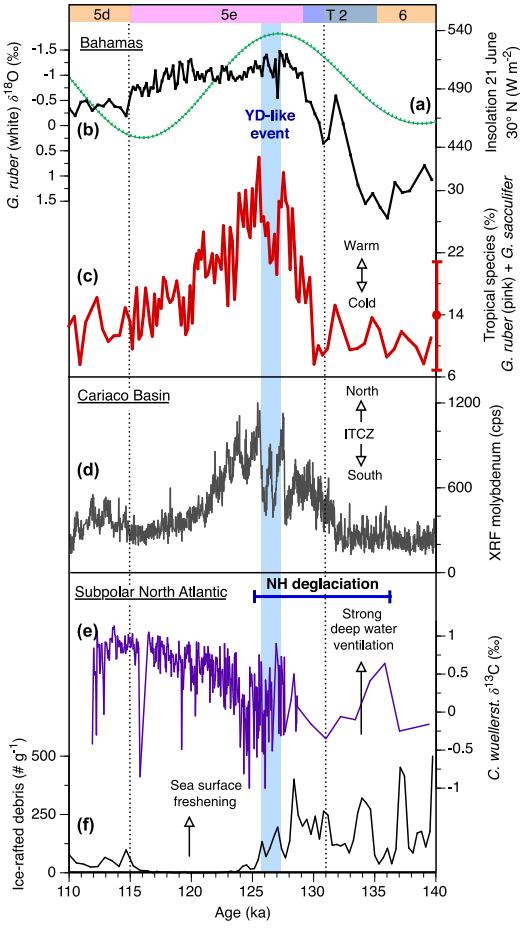

Figure 6. Comparison of proxy records from the tropical, subtropical and subpolar North Atlantic over the last interglacial cycle. **(b)** δ^{18}O values in *G. ruber* (white) in core MD99-2202 (Lantzsch et al., 2007). **(c)** Relative abundances of the tropical species *G. sacculifer* and *G. ruber* (pink) in core MD99-2202. **(d)** The molybdenum record from ODP Site 1002 (Gibson and Peterson, 2014). **(e)** δ^{13}C values measured in benthic foraminifera from core MD03-2664 (Galaasen et al., 2014, age model is from Zhuravleva et al., 2017b). **(f)** Ice-rafted debris in core PS1243 (Bauch et al., 2012, age model is from Zhuravleva et al., 2017b). Also shown is **(a)** boreal summer insolation (21 June, 30° N), computed with AnalySeries 2.0.8 (Paillard et al., 1996) using Laskar et al. (2004) data. Shown in **(c)** are modern relative abundances of *G. sacculifer* and *G. ruber* (pink) (average value $\pm 1\sigma$) around Bahama Bank, computed using the seven nearest samples from the Siccha and Kučera (2017) database. The blue band suggests a correlation of events (Younger Dryas-like cooling) across the tropical, subtropical and subpolar North Atlantic (see text). Dashed vertical lines frame MIS 5e. T2 represents Termination 2.

6.3 MIS 5e climate in the subtropics: orbital versus subpolar forcing

Various environmental changes within the mixed layer (SST, SSS and nutrients) can account for proportional change in different *Globigerinoides* species (Fig. 5). *G. sacculifer* – it makes up less than 10 % of the planktic foraminiferal assemblage around the LBB today (Siccha and Kučera, 2017) – is abundant in the Caribbean Sea and tropical Atlantic and is commonly used as a tracer of tropical waters and geographical shifts of the ITCZ (Poore et al., 2003; Vautravers et al., 2007). Furthermore, *G. ruber* (pink) also shows rather coherent abundance maxima in the tropics, while no such affinity is observed for *G. ruber* (white) and *G. conglobatus* (Siccha and Kučera, 2017; Schiebel and Hemleben, 2017). Therefore, fluctuations in relative abundances of *G. sacculifer* and *G. ruber* (pink) are put forward here as representing a warm "tropical" end-member (Fig. 1b).

Relative abundances of the tropical foraminifera (hereafter *G. ruber* (pink) and *G. sacculifer* calculated together) in our core suggest an early thermal maximum (between ~ 129 and 124 ka), which agrees well with the recent compilation of global MIS 5e SST (Hoffman et al., 2017). The sea surface warming could be related to a northward expansion of the Atlantic Warm Pool (Ziegler et al., 2008), in response to a northern location of the mean annual position of the ITCZ. The latter shift in the atmospheric circulation is explained by the particularly strong Northern Hemisphere insolation during early MIS 5e (Fig. 6), resulting in a cross-latitudinal thermal gradient change, which forced the ITCZ towards a

warming (Northern) Hemisphere (Schneider et al., 2014). A northern location of the mean annual position of the ITCZ during the first phase of the last interglacial is supported by the XRF data from the Cariaco Basin, which shows the highest accumulation of the redox-sensitive element molybdenum (Mo) during early MIS 5e (Fig. 6). At that latter location high Mo content is found in sediments deposited under anoxic conditions, which only occurs during warm interstadial periods associated with an ITCZ that has shifted to the north (Gibson and Peterson, 2014).

Further, our data reveal a millennial-scale cooling/salinification event at ~ 127 ka, characterized by decreased proportions of the tropical foraminifera and elevated planktic δ^{18}O values (Fig. 6). The fact that this abrupt cooling characterized the entire upper water column at the onset of the event is indicated by the reoccurrence of the cold-water species *G. inflata* coincident with the brief positive excursions in δ^{18}O values in the shallow and thermocline-dwelling foraminifera (Fig. 4). Simultaneously, the XRF record from the Cariaco Basin reveals a stadial-like Mo-depleted (i.e., southward ITCZ shift) interval (Fig. 6). The close similarity between the tropical-species record from the Bahamas and the XRF data from the Cariaco Basin supports the hypothesis that annual displacements of the ITCZ are also documented in our faunal counts. Thus, a southward shift in the mean annual position of the ITCZ at ~ 127 ka could have restricted the influence of the Atlantic Warm Pool in the Bahama region, reducing SST and possibly increasing SSS, and in turn, affecting the foraminiferal assemblage. Moreover, because the aforementioned abrupt climatic shift at ~ 127 ka cannot be reconciled with insolation changes, other forcing factors at play during early MIS 5e should be considered. Studies from the low-latitude Atlantic reveal a strong coupling between the ITCZ position and the AMOC strength associated with millennial-scale climatic variability (Rühlemann et al., 1999; Schmidt et al., 2006a; Carlson et al., 2008). In particular, model simulations and proxy data suggest that freshwater inputs as well as sea-ice extent in the (sub)polar North Atlantic can affect the ITCZ position through feedbacks on the thermohaline circulation and associated changes in the cross-latitudinal heat redistribution (e.g., Chiang et al., 2003; Broccoli et al., 2006; Gibson and Peterson, 2014).

It is well-established that the deepwater overflow from the Nordic Seas, which constitutes the deepest southward-flowing branch of the AMOC today (e.g., Stahr and Sanford, 1999), only strengthened (deepened) during the second phase of MIS 5e (at ~ 124 ka), and after the deglacial meltwater input into the region ceased (Hodell et al., 2009; Barker et al., 2015). Nevertheless, several studies show that the deep-water ventilation and presumably the AMOC abruptly recovered at the beginning of MIS 5e, at ~ 129 ka (Fig. 6), possibly linked to a deepened winter convection in the northwestern Atlantic (Adkins et al., 1997; Galaasen et al., 2014; Deaney et al., 2017). Accordingly, the resumption of the AMOC could have added to a meridional redistribution of the incoming solar heat, changing the cross-latitudinal thermal gradient and, thus, contributing to the inferred "orbitally driven" northward ITCZ shift during early MIS 5e (see above). In turn, the millennial-scale climatic reversal between 127 and 126 ka could have been related to the known reductions of deep water ventilation (Galaasen et al., 2014; Deaney et al., 2017), possibly attributed to a brief increase in the freshwater input into the subpolar North Atlantic and accompanied by a regional sea surface cooling (Irvalı et al., 2012; Zhuravleva et al., 2017b).

A corresponding cooling and freshening event, referred to here and elsewhere as a Younger Dryas-like event, is captured in some high- and mid-latitude North Atlantic records (Sarnthein and Tiedemann, 1990; Bauch et al., 2012; Irvalı et al., 2012; Schwab et al., 2013; Govin et al., 2014; Jiménez-Amat and Zahn, 2015). In combination with the Younger Dryas-like cooling and the reduction (shallowing) in the North Atlantic Deep Water formation, an increase in the Antarctic Bottom Water influence is revealed in the Southern Ocean sediments, arguing for the existence of an "interglacial" bipolar seesaw (Hayes et al., 2014). The out-of-phase climatic relationship between high northern and high southern latitudes, typical for the last glacial termination (Barker et al., 2009), could be attributed to a strong sensitivity of the transitional climatic regime of early MIS 5e due to persistent high-latitude freshening (i.e., continuing deglaciation, Fig. 6) and suppressed overturning in the Nordic Seas (Hodell et al., 2009). This assumption seems of crucial importance as it might help explain the relatively "late" occurrence of the Younger Dryas-like event during the last interglacial when compared to the actual Younger Dryas during the last deglaciation (Bauch et al., 2012). The recognition of the transitional phase during early MIS 5e is not new, but only a few authors have pointed out its importance for understanding the last interglacial climatic evolution beyond the subpolar regions (e.g., Govin et al., 2012; Schwab et al., 2013; Kandiano et al., 2014).

As insolation forcing decreased during late MIS 5e and the ITCZ gradually moved southward, the white variety of *G. ruber* started to dominate the assemblage (Fig. 5), arguing for generally colder sea surface conditions in the Bahama region. The inferred broad salinity tolerance of this species, also to neritic conditions (Bé and Tolderlund, 1971; Schmuker and Schiebel, 2002), was used in some studies to link high proportions of *G. ruber* (pink and white varieties) with low SSS (Vautravers et al., 2007; Kandiano et al., 2012). However, the plots of the global distribution pattern of *G. ruber* (white) and *G. ruber* (pink) suggest that when relative abundances of these two species are approaching maximum values (40 % and 10 %, respectively), the SSSs would be higher for specimens of the white variety of *G. ruber* (Hilbrecht, 1996). Therefore, the strongly dominating white versus pink *G. ruber* variety observed in our records during late MIS 5e could

be linked not only to decreasing SSTs, but also to elevated SSSs.

In their study from the western STG, Bahr et al. (2013) also reconstructed sea surface salinification during late MIS 5e in response to enhanced wind stress at times of deteriorating high-latitude climate and increasing meridional gradients. Accordingly, our isotopic and faunal data (note the abrupt decrease in *G. sacculifer* proportion at 120 ka; Fig. 5) suggest a pronounced climatic shift that could be attributed to the so-called "neoglaciation", consistent with the sea surface cooling in the western Nordic Seas and the Labrador Sea (Van Nieuwenhove et al., 2013; Irvalı et al., 2016) as well as with a renewed growth of terrestrial ice (Fronval and Jansen, 1997; Zhuravleva et al., 2017a).

7 Conclusions

New faunal, isotopic and XRF evidence from the Bahama region was studied for past subtropical climatic evolution, with special attention given to (1) the mechanisms controlling the planktic foraminiferal assemblage and (2) the climatic feedbacks between low and high latitudes.

During late MIS 6 and glacial termination, strongly reduced δ^{18}O gradients between surface- and thermocline-dwelling foraminifera suggest decreased water column stratification, which promoted high relative abundances of *G. truncatulinoides* (dex) and *G. inflata*. The lowered upper water column stratification, in turn, could be a result of sea surface cooling/salinification and intensified trade wind strength at times when the ITCZ was shifted far to the south.

Computed together, relative abundances of the tropical foraminifera *G. sacculifer* and *G. ruber* (pink) agree well with the published ITCZ-related Cariaco Basin record (Gibson and Peterson, 2014), suggesting a climatic coupling between the regions. Based on these data, a northward/southward displacement of the mean annual ITCZ position, in line with strong/weak Northern Hemisphere insolation, could be inferred for early/late MIS 5e.

Crucially, an abrupt Younger Dryas-like sea surface cooling/salinification event at $\sim$ 127 ka intersected the early MIS 5e warmth (between $\sim$ 129 and 124 ka) and could be associated with a sudden southward displacement of the ITCZ. Furthermore, this atmospheric shift could also be related to a millennial-scale instability in the ocean overturning, supporting a cross-latitudinal teleconnection that influenced the subtropical climate via ocean–atmospheric forcing. These observations lead to the inference that the persistent ocean freshening in the high northern latitudes (i.e., continuing deglaciation) and the resulting unstable deep water overturning during early MIS 5e accounted for a particularly sensitive climatic regime, associated with the abrupt warm–cold switches that could be traced across various oceanic basins.

Data availability. All data are available in the online database PANGAEA (https://doi.pangaea.de/10.1594/PANGAEA.893369, Zhuravleva et al., 2018).

Competing interests. The authors declare that they have no conflict of interest.

Acknowledgements. We wish to thank Hendrik Lantzsch and John J. G. Reijmer for providing us with the sediment core and data from core MD99-2202, Sebastian Fessler for performing measurements on stable isotopes, Samuel Müller and Dieter Garbe-Schönberg for technical assistance during XRF scanning, Julia Lübbers for her help with sample preparation, and Evgenia Kandiano for the introduction to tropical foraminiferal assemblages. Comments by André Bahr and one anonymous reviewer greatly improved the paper. Anastasia Zhuravleva acknowledges funding from the German Research Foundation (DFG grant no. BA1367/12-1).

The article processing charges for this open-access publication were covered by a research center of the Helmholtz Association.

Edited by: Alessio Rovere
Reviewed by: André Bahr and one anonymous referee

References

Adkins, J. F., Boyle, E. A., Keigwin, L., and Cortijo, E.: Variability of the North Atlantic thermohaline circulation during the last interglacial period, Nature, 390, 154–156, https://doi.org/10.1038/36540, 1997.

Arbuszewski, J. A., deMenocal, P. B., Cléroux, C., Bradtmiller, L., and Mix, A.: Meridional shifts of the Atlantic intertropical convergence zone since the Last Glacial Maximum, Nature Geosci., 6, 959–962, https://doi.org/10.1038/ngeo1961, 2013.

Bahr, A., Nürnberg, D., Schönfeld, J., and Garbe-Schönberg, D.: Hydrological variability in Florida Straits during Marine Isotope Stage 5 cold events, Paleoceanography, 26, PA2214, https://doi.org/10.1029/2010PA002015, 2011.

Bahr, A., Nürnberg, D., Karas, C., and Grützner, J.: Millennial-scale versus long-term dynamics in the surface and subsurface of the western North Atlantic Subtropical Gyre during Marine Isotope Stage 5, Glob. Planet. Change, 111, 77–87, https://doi.org/10.1016/j.gloplacha.2013.08.013, 2013.

Bahr, A., Jiménez-Espejo, F. J., Kolasinac, N., Grunert, P., Hernández-Molina, F. J., Röhl, U., Voelker, A. H. L., Escutia, C., Stow, D. A. V., Hodell, D., and Alvarez-Zarikian, C. A.: Deciphering bottom current velocity and paleoclimate signals from contourite deposits in the Gulf of Cádiz during the last 140 kyr: An inorganic geochemical approach, Geochem. Geophy. Geosy., 15, 3145–3160, https://doi.org/10.1002/2014GC005356, 2014.

Barker, S., Diz, P., Vautravers, M. J., Pike, J., Knorr, G., Hall, I. R., and Broecker, W. S.: Interhemispheric Atlantic seesaw response during the last deglaciation, Nature, 457, 1097, https://doi.org/10.1038/nature07770, 2009.

Barker, S., Chen, J., Gong, X., Jonkers, L., Knorr, G., and Thornalley, D.: Icebergs not the trigger for North Atlantic cold events, Nature 520, 333–336, https://doi.org/10.1038/nature14330, 2015.

Bauch, H. A., Kandiano, E. S., and Helmke, J. P.: Contrasting ocean changes between the subpolar and polar North Atlantic during the past 135 ka, Geophys. Res. Lett., 39, L11604, https://doi.org/10.1029/2012GL051800, 2012.

Bé, A. W. H. and Tolderlund, D. S.: Distribution and ecology of living planktonic foraminifera in surface waters of the Atlantic and Indian Oceans, edited by: Funnel, B. and Riedel, W. R., The Micropalaeontology of Oceans, Cambridge University Press, Cambridge, 105–149, 1971.

Boli, H. M. and Saunders, J. B.: Oligocene to Holocene low latitude planktic foraminifera, in: Plankton Stratigraphy, edited by: Bolli, H. M., Saunders, J. B., and Perch-Nielsen, K., Cambridge University Press, New York, 155–262, 1985.

Broccoli, A. J., Dahl, K. A., and Stouffer, R. J.: Response of the ITCZ to Northern Hemisphere cooling, Geophys. Res. Lett., 33, L01702, https://doi.org/10.1029/2005GL024546, 2006.

Carew, J. L. and Mylroie, J. E.: Quaternary tectonic stability of the Bahamian archipelago: evidence from fossil coral reefs and flank margin caves, Quaternary Sci. Rev., 14, 145–153, https://doi.org/10.1016/0277-3791(94)00108-N, 1995.

Carew, J. L. and Mylroie, J. E.: Geology of the Bahamas, in: Geology and Hydrogeology of Carbonate Islands, Develop. Sediment., 54, Elsevier Science, 91–139, 1997.

Carlson, A. E., Oppo, D. W., Came, R. E., LeGrande, A. N., Keigwin, L. D., and Curry, W. B.: Subtropical Atlantic salinity variability and Atlantic meridional circulation during the last deglaciation, Geology, 36, 991–994, https://doi.org/10.1130/G25080A.1, 2008.

Chabaud, L.: Modèle stratigraphique et processus sédimentaires au Quaternaire sur deux pentes carbonatées des Bahamas (leeward et windward), Doctoral dissertation, Université de Bordeaux, Francais, 2016.

Chabaud, L., Ducassou, E., Tournadour, E., Mulder, T., Reijmer, J. J. G., Conesa, G., Giraudeau, J., Hanquiez, V., Borgomano, J., and Ross, L.: Sedimentary processes determining the modern carbonate periplatform drift of Little Bahama Bank, Mar. Geol., 378, 213–229, https://doi.org/10.1016/j.margeo.2015.11.006, 2016.

Chang, P., Zhang, R., Hazeleger, W., Wen, C., Wan, X., Ji, L., Haarsma, R. J., Breugem, W.-P., and Seidel, H.: Oceanic link between abrupt changes in the North Atlantic Ocean and the African monsoon, Nat. Geosci., 1, 444–448, https://doi.org/10.1038/ngeo218, 2008.

Chiang, J. C. H., Biasutti, M., and Battisti, D. S.: Sensitivity of the Atlantic Intertropical Convergence Zone to Last Glacial Maximum boundary conditions, Paleoceanography, 18, 1094, https://doi.org/10.1029/2003PA000916, 2003.

Chiang, J. C. H., Cheng, W., and Bitz, C. M.: Fast teleconnections to the tropical Atlantic sector from Atlantic thermohaline adjustment, Geophys. Res. Lett., 35, L07704, https://doi.org/10.1029/2008GL033292, 2008.

Cléroux, C., Cortijo, E., Duplessy, J., and Zahn, R.: Deep-dwelling foraminifera as thermocline temperature recorders, Geochem. Geophy. Geosy., 8, Q04N11, https://doi.org/10.1029/2006GC001474, 2007.

Cortijo, E., Lehman, S., Keigwin, L., Chapman, M., Paillard, D., and Labeyrie, L.: Changes in Meridional Temperature and Salinity Gradients in the North Atlantic Ocean (30°–72° N) during the Last Interglacial Period, Paleoceanography, 14, 23–33, https://doi.org/10.1029/1998PA900004, 1999.

Deaney, E. L., Barker, S., and van de Flierdt, T.: Timing and nature of AMOC recovery across Termination 2 and magnitude of deglacial CO_2 change, Nat. Commun., 8, 14595, https://doi.org/10.1038/ncomms14595, 2017.

Droxler, A. W. and Schlager, W.: Glacial versus interglacial sedimentation rates and turbidite frequency in the Bahamas, Geology, 13, 799–802, 1985.

Dutton, A., Carlson, A. E., Long, A. J., Milne, G. A., Clark, P. U., DeConto, R., Horton, B. P., Rahmstorf, S., and Raymo, M. E.: Sea-level rise due to polar ice-sheet mass loss during past warm periods, Science, 349, 6244, https://doi.org/10.1126/science.aaa4019, 2015.

Ericson, D. B. and Wollin, G.: Pleistocene climates and chronology in deep-sea sediments, Science, 162, 1227–1234, 1968.

Fronval, T. and Jansen, E.: Eemian and Early Weichselian (140–60 ka) Paleoceanography and paleoclimate in the Nordic Seas with comparisons to Holocene conditions, Paleoceanography, 12, 443–462, https://doi.org/10.1029/97PA00322, 1997.

Galaasen, E. V., Ninnemann, U. S., Irvalı, N., Kleiven, H. (Kikki) F., Rosenthal, Y., Kissel, C., and Hodell, D. A.: Rapid Reductions in North Atlantic Deep Water During the Peak of the Last Interglacial Period, Science, 343, 1129, https://doi.org/10.1126/science.1248667, 2014.

Gibson, K. A. and Peterson, L. C.: A 0.6 million year record of millennial-scale climate variability in the tropics, Geophys. Res. Lett., 41, 969–975, https://doi.org/10.1002/2013GL058846, 2014.

Govin, A., Braconnot, P., Capron, E., Cortijo, E., Duplessy, J.-C., Jansen, E., Labeyrie, L., Landais, A., Marti, O., Michel, E., Mosquet, E., Risebrobakken, B., Swingedouw, D., and Waelbroeck, C.: Persistent influence of ice sheet melting on high northern latitude climate during the early Last Interglacial, Clim. Past, 8, 483–507, https://doi.org/10.5194/cp-8-483-2012, 2012.

Govin, A., Varma, V., and Prange, M.: Astronomically forced variations in western African rainfall (21°N–20°S) during the Last Interglacial period, Geophys. Res. Lett., 41, 2117–2125, https://doi.org/10.1002/2013GL058999, 2014.

Govin, A., Capron, E., Tzedakis, P. C., Verheyden, S., Ghaleb, B., Hillaire-Marcel, C., St-Onge, G., Stoner, J. S., Bassinot, F., Bazin, L., Blunier, T., Combourieu-Nebout, N., El Ouahabi, A., Genty, D., Gersonde, R., Jiménez-Amat, P., Landais, A., Martrat, B., Masson-Delmotte, V., Parrenin, F., Seidenkrantz, M.-S., Veres, D., Waelbroeck, C., and Zahn, R.: Sequence of events from the onset to the demise of the Last Interglacial: Evaluating strengths and limitations of chronologies used in climatic archives, Quaternary Sci. Rev., 129, 1–36, https://doi.org/10.1016/j.quascirev.2015.09.018, 2015.

Groeneveld, J. and Chiessi, C. M.: Mg/Ca of *Globorotalia inflata* as a recorder of permanent thermocline temperatures in the South Atlantic, Paleoceanography, 26, PA2203, https://doi.org/10.1029/2010PA001940, 2011.

Hayes, C. T., Martínez-García, A., Hasenfratz, A. P., Jaccard, S. L., Hodell, D. A., Sigman, D. M., Haug, G. H., and Anderson, R. F.: A stagnation event in the deep South Atlantic

during the last interglacial period, Science, 346, 1514–1517, https://doi.org/10.1126/science.1256620, 2014.

Hearty, P. J. and Neumann, A. C.: Rapid sea level and climate change at the close of the Last Interglaciation (MIS 5e): evidence from the Bahama Islands, Quaternary Sci. Rev., 20, 1881–1895, https://doi.org/10.1016/S0277-3791(01)00021-X, 2001.

Helmke, J. P., Bauch, H. A., Röhl, U., and Kandiano, E. S.: Uniform climate development between the subtropical and subpolar Northeast Atlantic across marine isotope stage 11, Clim. Past, 4, 181–190, https://doi.org/10.5194/cp-4-181-2008, 2008.

Hennekam, R. and de Lange, G.: X-ray fluorescence core scanning of wet marine sediments: methods to improve quality and reproducibility of high-resolution paleoenvironmental records, Limnol. Oceanogr., 10, 991–1003, https://doi.org/10.4319/lom.2012.10.991, 2012.

Hilbrecht, H.: Extant planktic foraminifera and the physical environment in the Atlantic and Indian Oceans: an atlas based on Climap and Levitus (1982) data. Mitteilungen aus dem Geologischen Institut der Eidgen. Technischen Hochschule und der Universität Zürich, Neue Folge, Zürich, 93 pp., 1996.

Hodell, D. A., Minth, E. K., Curtis, J. H., McCave, I. N., Hall, I. R., Channell, J. E. T., and Xuan, C.: Surface and deep-water hydrography on Gardar Drift (Iceland Basin) during the last interglacial period, Earth Planet. Sc. Lett,. 288, 10–19, https://doi.org/10.1016/j.epsl.2009.08.040, 2009.

Hoffman, J. S., Clark, P. U., Parnell, A. C., and He, F.: Regional and global sea-surface temperatures during the last interglaciation, Science, 355, 276–279, https://doi.org/10.1126/science.aai8464, 2017.

Irvalı, N., Ninnemann, U. S., Galaasen, E. V., Rosenthal, Y., Kroon, D., Oppo, D. W., Kleiven, H. F., Darling, K. F., and Kissel, C.: Rapid switches in subpolar North Atlantic hydrography and climate during the Last Interglacial (MIS 5e), Paleoceanography, 27, PA2207, https://doi.org/10.1029/2011PA002244, 2012.

Irvalı, N., Ninnemann, U. S., Kleiven, H. (Kikki) F., Galaasen, E. V., Morley, A., and Rosenthal, Y.: Evidence for regional cooling, frontal advances, and East Greenland Ice Sheet changes during the demise of the last interglacial, Quaternary Sci. Rev., 150, 184–199, https://doi.org/10.1016/j.quascirev.2016.08.029, 2016.

Jentzen, A., Schönfeld, J., and Schiebel, R.: Assessment of the Effect of Increasing Temperature On the Ecology and Assemblage Structure of Modern Planktic Foraminifers in the Caribbean and Surrounding Seas, J. Foraminiferal Res., 48, 251–272, https://doi.org/10.2113/gsjfr.48.3.251, 2018.

Jiménez-Amat, P. and Zahn, R.: Offset timing of climate oscillations during the last two glacial-interglacial transitions connected with large-scale freshwater perturbation, Paleoceanography, 30, 768–788, https://doi.org/10.1002/2014PA002710, 2015.

Johns, W. E., Townsend, T. L., Fratantoni, D. M., and Wilson, W. D.: On the Atlantic inflow to the Caribbean Sea, Deep Sea Res. Pt I, 49, 211–243, https://doi.org/10.1016/S0967-0637(01)00041-3, 2002.

Jonkers, L. and Kučera, M.: Global analysis of seasonality in the shell flux of extant planktonic Foraminifera, Biogeosciences, 12, 2207–2226, https://doi.org/10.5194/bg-12-2207-2015, 2015.

Kandiano, E. S., Bauch, H. A., Fahl, K., Helmke, J. P., Röhl, U., Pérez-Folgado, M., and Cacho, I.: The meridional temperature gradient in the eastern North Atlantic during MIS 11 and its link to the ocean–atmosphere system, Palaeogeogr. Palaeoclimatol. Palaeoecol., 333–334, 24–39, https://doi.org/10.1016/j.palaeo.2012.03.005, 2012.

Kandiano, E. S., Bauch, H. A., and Fahl, K.: Last interglacial surface water structure in the western Mediterranean (Balearic) Sea: Climatic variability and link between low and high latitudes, Glob. Planet. Change, 123, 67–76, https://doi.org/10.1016/j.gloplacha.2014.10.004, 2014.

Lantzsch, H., Roth, S., Reijmer, J. J. G., and Kinkel, H.: Sea-level related resedimentation processes on the northern slope of Little Bahama Bank (Middle Pleistocene to Holocene), Sedimentology, 54, 1307–1322, https://doi.org/10.1111/j.1365-3091.2007.00882.x, 2007.

Laskar, J., Robutel, P., Joutel, F., Gastineau, M., Correia, A. C. M., and Levrard, B.: A long-term numerical solution for the insolation quantities of the Earth, Astron. Astrophys., 428, 261–285, https://doi.org/10.1051/0004-6361:20041335, 2004.

Levitus, S., Antonov, J. I., Baranova, O. K., Boyer, T. P., Coleman, C. L., Garcia, H. E., Grodsky, A. I., Johnson, D. R., Locarnini, R. A., and Mishonov, A. V.: The world ocean database, Data Sci. J., 12, WDS229-WDS234, https://doi.org/10.2481/dsj.WDS-041, 2013.

Lisiecki, L. E. and Stern, J. V.: Regional and global benthic $\delta^{18}O$ stacks for the last glacial cycle, Paleoceanography, 31, 1368–1394, https://doi.org/10.1002/2016PA003002, 2016.

Lohmann, G. P. and Schweitzer, P. N.: *Globorotalia truncatulinoides*' Growth and chemistry as probes of the past thermocline: 1. Shell size, Paleoceanography, 5, 55–75, https://doi.org/10.1029/PA005i001p00055, 1990.

Loulergue, L., Schilt, A., Spahni, R., Masson-Delmotte, V., Blunier, T., Lemieux, B., Barnola, J.-M., Raynaud, D., Stocker, T. F., and Chappellaz, J.: Orbital and millennial-scale features of atmospheric CH_4 over the past 800,000 years, Nature, 453, 383–386, https://doi.org/10.1038/nature06950, 2008.

Maslin, M., Sarnthein, M., Knaack, J. J., Grootes, P., and Tzedakis, C.: Intra-interglacial cold events: an Eemian-Holocene comparison. Geol. Soc., London, Special Publications, 131, 91–99, https://doi.org/10.1144/GSL.SP.1998.131.01.07, 1998.

Masson-Delmotte, V., Schulz, M., Abe-Ouchi, A., Beer, J., Ganopolski, A., González Rouco, J. F., Jansen, E., Lambeck, K., Luterbacher, J., and Naish, T.: Information from paleoclimate archives, edited by: Stocker, T. F., Qin, D., Plattner, G.-K., Tignor, M., Allen, S. K., Boschung, J., Nauels, A., Xia, Y., Bex, V., and Midgley, P. M., Climate Change 2013: The Physical Science Basis. Contribution of Working Group I to the Fifth Assessment Report of the Intergovernmental Panel on Climate Change, 383–464, 2013.

Morse, J. W. and MacKenzie, F. T.: Geochemistry of sedimentary carbonates, Elsevier, 1990.

Muhs, D. R., Budahn, J. R., Prospero, J. M., and Carey, S. N.: Geochemical evidence for African dust inputs to soils of western Atlantic islands: Barbados, the Bahamas, and Florida, J. Geophys. Res.-Earth Surf., 112, F02009, https://doi.org/10.1029/2005JF000445, 2007.

Mulitza, S., Dürkoop, A., Hale, W., Wefer, G., and Niebler, H. S.: Planktonic foraminifera as recorders of past surface-water stratification, Geology, 25, 335–338, https://doi.org/10.1130/0091-7613(1997)025<0335:PFAROP>2.3.CO;2, 1997.

Neumann, A. C. and Land, L. S.: Lime mud deposition and calcareous algae in the Bight of Abaco, Bahamas; a budget, J. Sediment. Res., 45, 763–786, 1975.

NGRIP community members: High-resolution record of Northern Hemisphere climate extending into the last interglacial period, Nature, 431, 147–151, https://doi.org/10.1038/nature02805, 2004.

Paillard, D., Labeyrie, L., and Yiou, P.: Macintosh Program performs time-series analysis, Eos Trans AGU, 77, 379–379, https://doi.org/10.1029/96EO00259, 1996.

Peterson, L. C. and Haug, G. H.: Variability in the mean latitude of the Atlantic Intertropical Convergence Zone as recorded by riverine input of sediments to the Cariaco Basin (Venezuela), Palaeogeogr. Palaeoclimatol. Palaeoecol., 234, 97–113, https://doi.org/10.1016/j.palaeo.2005.10.021, 2006.

Poore, R. Z., Dowsett, H. J., Verardo, S., and Quinn, T. M.: Millennial- to century-scale variability in Gulf of Mexico Holocene climate records, Paleoceanography, 18, 1048, https://doi.org/10.1029/2002PA000868, 2003.

Richter, T. O., van der Gaast, S., Koster, B., Vaars, A., Gieles, R., de Stigter, H. C., De Haas, H., and van Weering, T. C. E.: The Avaatech XRF Core Scanner: technical description and applications to NE Atlantic sediments, Geol. Soc. London, Special Publications, 267, 39–50, https://doi.org/10.1144/GSL.SP.2006.267.01.03, 2006.

Roth, S. and Reijmer, J. J. G.: Holocene Atlantic climate variations deduced from carbonate periplatform sediments (leeward margin, Great Bahama Bank), Paleoceanography, 19, PA1003, https://doi.org/10.1029/2003PA000885, 2004.

Roth, S. and Reijmer, J. J. G.: Holocene millennial to centennial carbonate cyclicity recorded in slope sediments of the Great Bahama Bank and its climatic implications, Sedimentology, 52, 161–181, https://doi.org/10.1111/j.1365-3091.2004.00684.x, 2005.

Rühlemann, C., Mulitza, S., Müller, P. J., Wefer, G., and Zahn, R.: Warming of the tropical Atlantic Ocean and slowdown of thermohaline circulation during the last deglaciation, Nature, 402, 511–514, https://doi.org/10.1038/990069, 1999.

Sarnthein, M. and Tiedemann, R.: Younger Dryas-style cooling events at glacial terminations I-VI at ODP site 658: Associated benthic δ^{13}C anomalies constrain meltwater hypothesis, Paleoceanogr. Paleoclimatol., 5, 1041–1055, https://doi.org/10.1029/PA005i006p01041, 1990.

Schiebel, R. and Hemleben, C.: Planktic Foraminifers in the Modern Ocean, Springer, 2017.

Schlager, W., Reijmer, J. J. G., and Droxler, A.: Highstand Shedding of Carbonate Platforms, J. Sedim. Res., 64B, 270–281, 1994.

Schlitzer, R.: Ocean Data View, software available at: http://odv.awi.de, last access: June 2017.

Schmidt, M. W., Vautravers, M. J., and Spero, H. J.: Rapid subtropical North Atlantic salinity oscillations across Dansgaard–Oeschger cycles, Nature, 443, 561–564, https://doi.org/10.1038/nature05121, 2006a.

Schmidt, M. W., Vautravers, M. J., and Spero, H. J.: Western Caribbean sea surface temperatures during the late Quaternary, Geochem. Geophy. Geosy., 7, Q02P10, https://doi.org/10.1029/2005GC000957, 2006b.

Schmitz, W. J. and McCartney, M. S.: On the North Atlantic Circulation, Rev. Geophys., 31, 29–49, https://doi.org/10.1029/92RG02583, 1993.

Schmitz, W. J. and Richardson, P. L.: On the sources of the Florida Current, Deep Sea Res. Pt. A, 38, S379–S409, https://doi.org/10.1016/S0198-0149(12)80018-5, 1991.

Schmuker, B. and Schiebel, R.: Planktic foraminifers and hydrography of the eastern and northern Caribbean Sea, Mar. Micropal., 46, 387–403, https://doi.org/10.1016/S0377-8398(02)00082-8, 2002.

Schneider, T., Bischoff, T., and Haug, G. H.: Migrations and dynamics of the intertropical convergence zone, Nature, 513, 45–53, https://doi.org/10.1038/nature13636, 2014.

Schwab, C., Kinkel, H., Weinelt, M., and Repschläger, J.: A coccolithophore based view on paleoenvironmental changes in the open ocean mid-latitude North Atlantic between 130 and 48 ka BP with special emphasis on MIS 5e, Quaternary Sci. Rev., 81, 35–47, https://doi.org/10.1016/j.quascirev.2013.09.021, 2013.

Siccha, M. and Kučera, M.: ForCenS, a curated database of planktonic foraminifera census counts in marine surface sediment samples, Sci. Data, 4, 170109, https://doi.org/10.1038/sdata.2017.109, 2017.

Slowey, N. C. and Curry, W. B.: Glacial-interglacial differences in circulation and carbon cycling within the upper western North Atlantic, Paleoceanography, 10, 715–732, https://doi.org/10.1029/95PA01166, 1995.

Slowey, N. C., Wilber, R. J., Haddad, G. A., and Henderson, G. M.: Glacial-to-Holocene sedimentation on the western slope of Great Bahama Bank, Mar. Geol., 185, 165–176, https://doi.org/10.1016/S0025-3227(01)00295-X, 2002.

Stahr, F. R. and Sanford, T. B.: Transport and bottom boundary layerobservations of the North Atlantic Deep Western Boundary Current at the Blake Outer Ridge, Deep Sea Res. Pt. II, 46, 205–243, https://doi.org/10.1016/S0967-0645(98)00101-5, 1999.

Stirling, C., Esat, T., Lambeck, K., and McCulloch, M.: Timing and duration of the Last Interglacial: evidence for a restricted interval of widespread coral reef growth, Earth Planet. Sc. Lett., 160, 745–762, https://doi.org/10.1016/S0012-821X(98)00125-3, 1998.

Stramma, L. and Schott, F.: The mean flow field of the tropical Atlantic Ocean, Deep Sea Res. Pt II, 46, 279–303, https://doi.org/10.1016/S0967-0645(98)00109-X, 1999.

Tedesco, K., Thunell, R., Astor, Y., and Muller-Karger, F.: The oxygen isotope composition of planktonic foraminifera from the Cariaco Basin, Venezuela: Seasonal and interannual variations, Mar. Micropal., 62, 180–193, https://doi.org/10.1016/j.marmicro.2006.08.002, 2007.

Tjallingii, R., Röhl, U., Kölling, M., and Bickert, T.: Influence of the water content on X-ray fluorescence core-scanning measurements in soft marine sediments, Geochem. Geophy. Geosy., 8, Q02004, https://doi.org/10.1029/2006GC001393, 2007.

Van Nieuwenhove, N., Bauch, H. A., and Andruleit, H.: Multiproxy fossil comparison reveals contrasting surface ocean conditions in the western Iceland Sea for the last two interglacials, Palaeogeogr. Palaeoclimatol. Palaeoecol., 370, 247–259, https://doi.org/10.1016/j.palaeo.2012.12.018, 2013.

Vautravers, M. J., Shackleton, N. J., Lopez-Martinez, C., and Grimalt, J. O.: Gulf Stream variability during marine isotope stage 3, Paleoceanography, 19, PA2011, https://doi.org/10.1029/2003PA000966, 2004.

Vautravers, M. J., Bianchil, G., and Sackleton, N. J.: Subtropical NW Atlantic surface water variability during the last inter-

glacial, in: The Climate of Past Interglacials, edited by: Sirocko, F., Claussen, M., Sánches-Goñi, M. F., and Litt, T., Developm. in Quat. Sci., Elsevier, 289–303, https://doi.org/10.1016/S1571-0866(07)80045-5, 2007.

Vellinga, M. and Wood, R. A.: Global Climatic Impacts of a Collapse of the Atlantic Thermohaline Circulation, Clim. Change, 54, 251–267, https://doi.org/10.1023/A:1016168827653, 2002.

Wang, C. and Lee, S.: Atlantic warm pool, Caribbean low-level jet, and their potential impact on Atlantic hurricanes, Geophys. Res. Lett., 34, L12713, https://doi.org/10.1029/2006GL028579, 2007.

Wang, X., Auler, A. S., Edwards, R. L., Cheng, H., Cristalli, P. S., Smart, P. L., Richards, D. A., and Shen, C.-C.: Wet periods in northeastern Brazil over the past 210 kyr linked to distant climate anomalies, Nature, 432, 740–743, https://doi.org/10.1038/nature03067, 2004.

Williams, S. C.: Stratigraphy, Facies Evolution and Diagenesis of Late Cenozoic Lime-stones and Dolomites, Little Bahama Bank, Bahamas, Univ. Miami, Coral Gables FL, 1985.

Wilson, P. A. and Roberts, H. H.: Density cascading: off-shelf sediment transport, evidence and implications, Bahama Banks, J. Sedim. Res., 65, 45–56, 1995.

Yarincik, K. M., Murray, R. W., and Peterson, L. C.: Climatically sensitive eolian and hemipelagic deposition in the Cariaco Basin, Venezuela, over the past 578,000 years: Results from Al/Ti and K/Al, Paleoceanography, 15, 210–228, https://doi.org/10.1029/1999PA900048, 2000.

Zhang, R.: Anticorrelated multidecadal variations between surface and subsurface tropical North Atlantic, Geophys. Res. Lett., 34, L12713, https://doi.org/10.1029/2007GL030225, 2007.

Zhuravleva, A. and Bauch, H. A.: Paleoceanographic data from core MD99-2202, available at: https://doi.pangaea.de/10.1594/PANGAEA.893369, 2018.

Zhuravleva, A., Bauch, H. A., and Spielhagen, R. F.: Atlantic water heat transfer through the Arctic Gateway (Fram Strait) during the Last Interglacial, Glob. Planet. Change, 157, 232–243, https://doi.org/10.1016/j.gloplacha.2017.09.005, 2017a.

Zhuravleva, A., Bauch, H. A., and Van Nieuwenhove, N.: Last Interglacial (MIS5e) hydrographic shifts linked to meltwater discharges from the East Greenland margin, Quaternary Sci. Rev., 164, 95–109, https://doi.org/10.1016/j.quascirev.2017.03.026, 2017b.

Ziegler, M., Nürnberg, D., Karas, C., Tiedemann, R., and Lourens, L. J.: Persistent summer expansion of the Atlantic Warm Pool during glacial abrupt cold events, Nature Geosci., 1, 601–605, https://doi.org/10.1038/ngeo277, 2008.